pp. 278-290

Reprinted with change of pagination from
3rd International Rarefied Gas Dynamics Symposium, Vol. II, pp. 278-290, 1963 (N.Y. Academic Press, 1963)

; JPL-TR-32-442)

Technical Report No. 32-442

Low-Density Sphere Drag with Equilibrium and Nonequilibrium Wall Temperature

Harry Ashkenas

Reprint

[8] cont.

This paper presents results of one phase of research carried out at the Jet Propulsion Laboratory, California Institute of Technology, under Contract No. NAS 7-100, sponsored by the National Aeronautics and Space Administration.

(NASA

JET PROPULSION LABORATORY
CALIFORNIA INSTITUTE OF TECHNOLOGY
PASADENA, CALIFORNIA

August, 1963 14 15 refs

REPRINTED FROM
3rd INTERNATIONAL RAREFIED GAS DYNAMICS SYMPOSIUM, VOL. II

ACADEMIC PRESS, INC., NEW YORK, N. Y.

Low-Density Sphere Drag with Equilibrium and Nonequilibrium Wall Temperature

HARRY ASHKENAS
Jet Propulsion Laboratory, California Institute of Technology
Pasadena, California

ABST 2 30 50

The drag of a sphere in a supersonic low-density flow has been measured under both equilibrium and nonequilibrium surface temperature conditions. The simple deflection technique described by Wegener and Ashkenas (1961a) has been exploited to yield drag data for free stream Mach numbers between 1.8 and 4.4, free stream Reynolds numbers between 3 and 125, and free stream Knudsen numbers between 1 and 0.05. Radiation heating of the sphere models has produced wall temperatures as high as 1860° R (= 1033° K) resulting in wall-to-free-stream temperature ratios up to 15; the drag increase due to heating has been measured at up to 25% of the equilibrium wall temperature value.

Author

1. Introduction

The flow regime between continuum flow and free molecular flow has long been of interest to workers in the field of low-density gas dynamics. Solutions of the very simplest problems, however, have been hampered by ignorance of the role and nature of the parameters which must be included in any analysis. The present investigation was planned to provide experimental data which might be used to furnish some insight into the mechanism of the drag of a body operating at a Knudsen number that is neither high enough for complete free-molecular flow nor low enough for complete continuum flow. Previous sphere drag investigations, e.g., Kane (1951), Sherman (1951), Jensen (1951), Wegener and Ashkenas (1961a,b), and Sreekanth (1961) have, in general, been concerned with the drag of a sphere, the surface of which has been allowed to reach an equilibrium temperature; i.e., recovery temperature and/or

radiation environment (tunnel walls at room temperature) have been the principle sources of sphere heating, giving a wall-to-stagnation temperature ratio approximately equal to one. The present experiments have been concerned not only with the case where $T_w/T_0 \approx 1$, but also with $T_w/T_0 > 1$. Emphasis has been placed on providing a fairly large body of experimental drag data, over widely varying wall temperatures, in the hope that a consistent picture of the drag mechanism might be formed.

II. Apparatus and Methods

A. Wind Tunnel

The experiments were conducted in Leg 1 of the Low Density Gas Dynamics Facility of the California Institute of Technology Jet Propulsion Laboratory. This facility has been recently relocated and modified as shown in Fig. 1; the modifications have resulted in the extension of tunnel operation to higher mass flows than were possible with the arrangement depicted by Wegener and Ashkenas (1961b). The tunnel is a conventional open-return, open-jet, low-density wind tunnel powered by three oil-diffusion-ejector pumps with a total pumping capacity of 7300 liters/sec at 1μ Hg. Features of the tunnel include remote actuation of valves, as well as automated safety devices which allow unattended operation of the facility; the latter provision makes for little operating time loss due to pump warm-up.

Two nozzles were used for the present experiments; the first of these was a simple conical nozzle designed to operate at a nominal Mach number of 2. The second was a copy of the contoured Mach number 4 nozzle described by Sreekanth (1956). Both nozzles were externally wrapped with a copper coil, and the entire assembly cast into a cylinder of low-melting-point alloy. Liquid nitrogen pumped through the copper coil cooled the entire mass to $\sim$80° K and the resultant thinning of the nozzle wall boundary layers allowed testing with an isentropic core to lower densities than were possible with the nozzle walls at room temperature. The cooling scheme and initial calibration of the cooled nozzles are due to Russell (1962).

For both nozzles, calibration was effected with a pitot-tube in combination with a strain-gage, diaphragm-type pressure transducer. The pitot tubes used were of circular cross section and had a 10° ($\frac{1}{2}$ angle) external chamfer at the mouth. Viscous corrections for such a tube have been reported by Enkenhus (1957) and Ashkenas (1962).

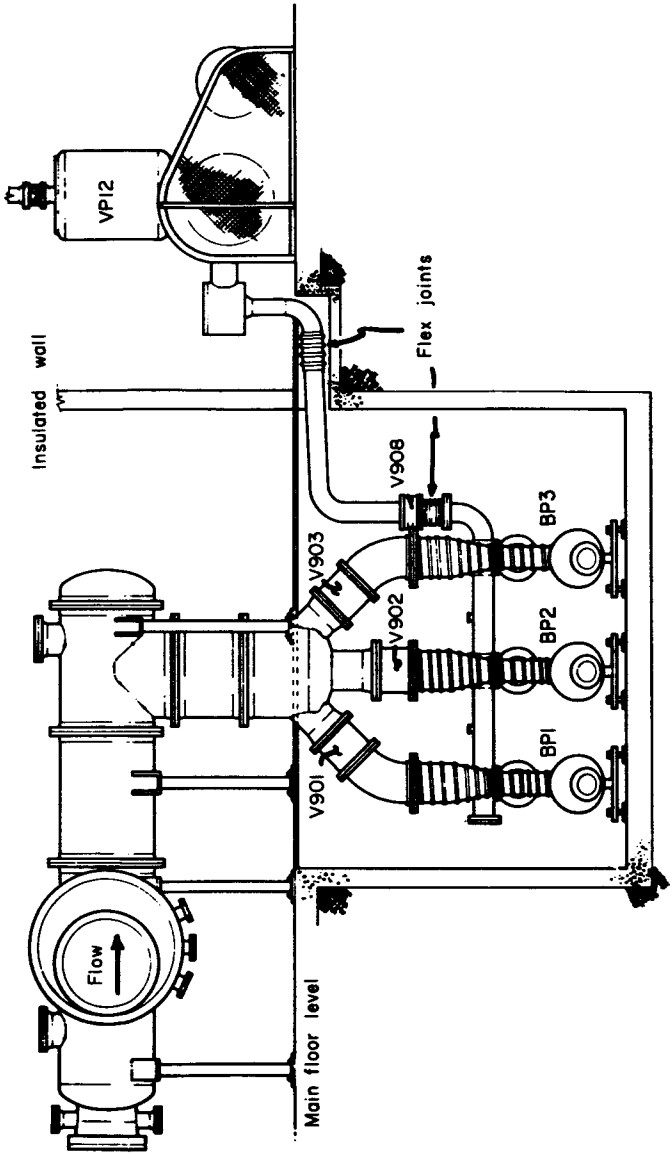

FIG. 1. Leg 1 of JPL low density wind tunnel.

Nozzle calibrations included the determination of that pressure in the tank containing the working section which minimized the Mach number gradient at the measuring station.

B. Models

Sphere models consisted of steel and bronze bearing balls $\frac{1}{32}$, $\frac{1}{16}$, and $\frac{1}{8}$ in. in diameter. Precision balls with diametral tolerances of ± 0.00001 in. and sphericity tolerance of 0.00001 in. were used in all cases. The sphere is suspended on a fine wire in the jet; damping is achieved by the addition of a second sphere immersed in silicone oil beneath the jet. Both tungsten wire and chromel-alumel wire were used for the suspension; diameters varied from 0.00015 to 0.0005 in. The flow geometry is shown in Fig. 2; Fig. 2 also sketches the methods of

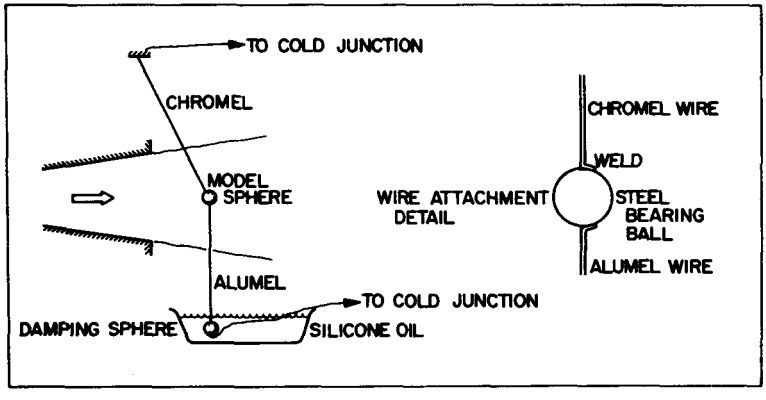

FIG. 2. Sphere drag flow geometry.

wire attachment and temperature measurement. The fine wires are welded to the sphere surface. For the thermocouple materials this results in the entire sphere acting as the thermojunction. Thus, the temperature measured is a bulk average; this is taken to be T_w, the wall temperature.

C. Sphere Heating

Radiation heating was used to control the temperature of the sphere. Two 8-mm movie projector lamps with built-in ellipsoidal reflectors were used in a manner similar to that described by Ostriker and Davey (1960). The combined rated output of the lamps was 300 watts. At this rating, the sphere surface temperature could be raised to about 1150° K. Since this is above the melting point of bronze, temperatures were

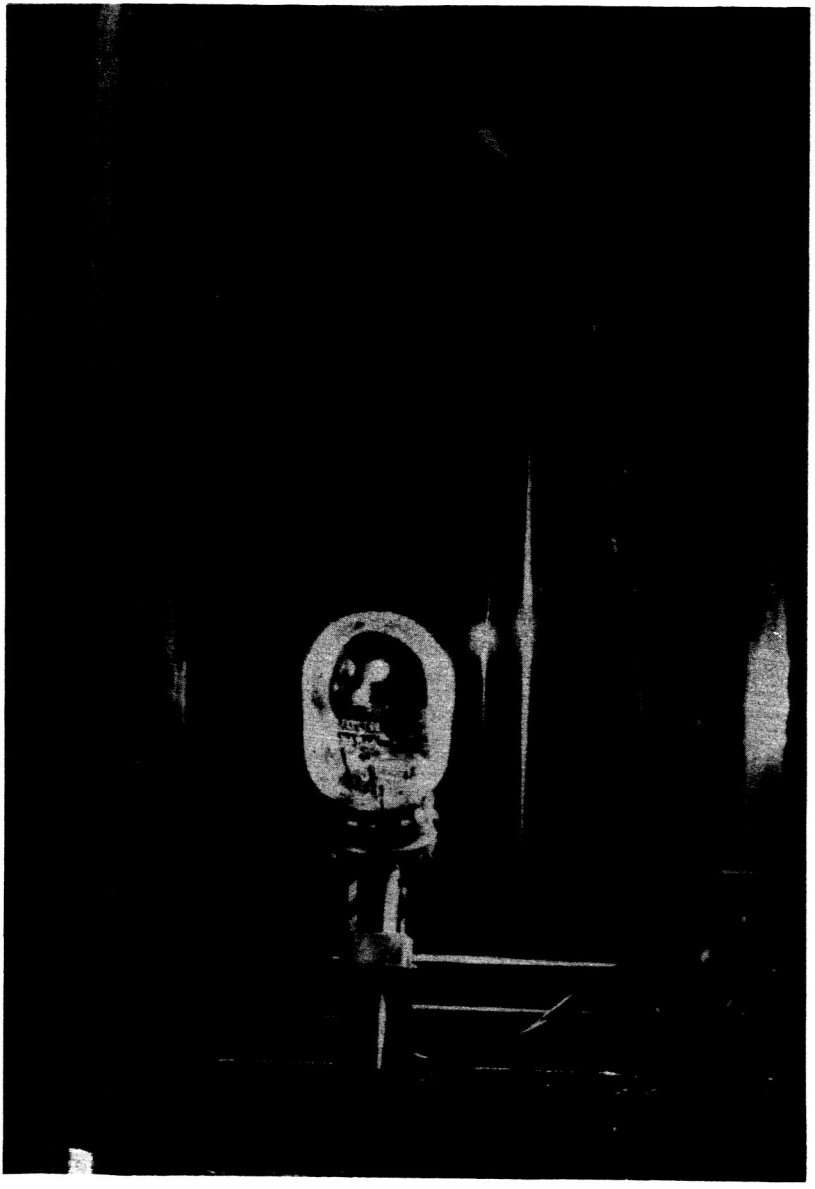

FIG. 3. Setup for heated sphere measurements.

restricted to less than 1000° K. The general arrangement of lamps, sphere and nozzle is shown in Fig. 3. The lamp bulbs are placed at the jet edges, and have no effect on the sphere drag, as evidenced by agreement between measurements with and without the bulbs in place.

Initial testing was done using the thermocouple wires as the support wires for the sphere; drag and wall temperatures were measured simultaneously. Subsequent tests with the smallest diameter (1/32 in.) sphere indicated that the tare drag of the smallest available thermocouple wire (0.0003 in.) was as great as the drag of the sphere itself. In order to eliminate these high tare runs, tungsten wires (0.00015 in. diam) were used for the suspensions. Sphere surface temperatures were determined by calibrating the power input to the heating lamps against the temperature of a given sphere suspended on thermocouple wire for all the flow conditions encountered during the drag measurement runs. This gives rise to some uncertainty as to the actual sphere temperature at which the drag measurements were made. It is estimated that this uncertainty is no more than $\pm 20°$ F.

III. Wire Tare Drag

The drag of the support wire must be determined in order to compute the drag of the sphere alone. The method of wire drag measurement has been reported in Wegener and Ashkenas (1961b). For the experiments reported here, additional measurements of the drag of a heated wire had to be made. Again, the photographic technique of Wegener and Ashkenas (1961b) was used. A chromel-alumel thermojunction formed of the suspension wires was placed at the measuring station and wire drag measured together with the temperature of the wire. The flow conditions and the lamp geometry were the same as those which obtained during the sphere drag experiments. Thus, although the wire had a nonuniform temperature distribution imposed upon it, the temperature loading was presumed the same as for the case of wire plus sphere. Finally, for ease of computation, an empirical equation was fitted to all the wire drag data for a given nozzle and this equation was used in the data reduction process. The two equations (for the two nozzles used) are:

For $M \approx 2$ nozzle:

$$D_w = k_d q_\infty T_w^{0.12}(0.250 M_\infty - 0.299)$$

For $M \approx 4$ nozzle:

$$D_w = k_d q_w T_w^{0.145}\ (0.458 M_\infty - 0.829)$$

Here T_w is the measured wire temperature, °R; M_∞ and q_∞ are the free stream Mach number and free stream dynamic pressure, respectively. The constant k_d in each of these equations was arbitrarily chosen to force the data for each different wire diameter to coincide. The departure of the measured wire drag from the empirical equations given above is of the order of $\pm 10\%$; for this reason, the wire diameter is chosen so that the wire drag never exceeds 30% of the total drag. Thus, errors in the sphere drag data due to uncertainties in the tare drag should not exceed $\pm 3\%$.

IV. Experimental Results and Discussion

The data for the sphere drag have been reduced by the methods described in Wegener and Ashkenas (1961b) to the form of C_D, the drag coefficient. Note is made here of the fact that the diameter of the sphere used in calculating the drag coefficient included the effects of thermal expansion. At the highest temperatures this correction represents a 2% change in the effective area of the sphere.

The sphere drag data are shown graphically in Figs. 4 and 5. Data obtained at $M \approx 2$ are shown in Fig. 4; those at $M \approx 4$, in Fig. 5. In these two figures, the drag coefficient is shown as a function of the Reynolds number at the wall, where

$$\mathrm{Re}_w = \frac{\rho_\infty U_\infty d}{\mu_w}$$

i.e., the Reynolds number based on free-stream mass flow, and viscosity evaluated at the wall temperature. Each of the curves in Figs. 4 and 5 represents a single free-stream condition; thus, M_∞, Re_∞, and Kn_∞ are constant along any one of the curves, as noted in the table on each figure. The variation in C_D and Re_w along each curve is due solely to the variation in the temperature of the sphere. Along each curve, decreasing Re_w represents increasing wall temperature. The effect of the increasing temperature is to increase the drag of the sphere.

The mechanism whereby heating the wall of the sphere results in a drag increase is not clear. That an increase is to be expected is evident. Consider the case of viscous, continuum flow: here, heating the wall increases the fluid viscosity giving rise to higher skin friction and thus increasing the drag. If we take the completely free molecular flow view, heating the wall of the body results in reflected molecules leaving the surface with greater energy than at incidence (assuming that the reflec-

tion process is not completely specular) and thus again, wall heating produces a drag increase.

To date, this writer has been unable to find a rational correlation parameter for the data shown in Figs. 4 and 5. The use of Re_w as the

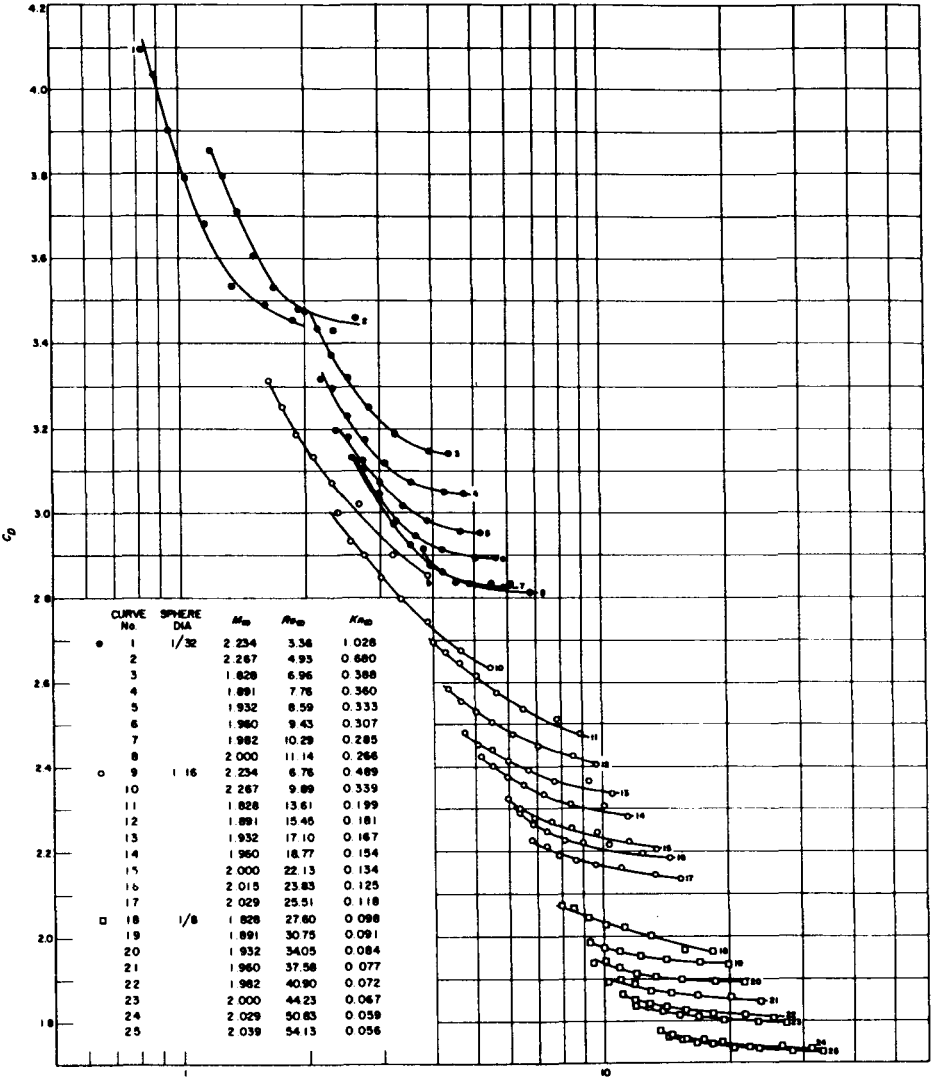

	CURVE No.	SPHERE DIA	M_∞	Re_∞	K_{n_∞}
●	1	1/32	2.234	3.36	1.028
	2		2.267	4.93	0.680
	3		1.828	6.96	0.388
	4		1.891	7.76	0.360
	5		1.932	8.59	0.333
	6		1.960	9.43	0.307
	7		1.982	10.29	0.285
	8		2.000	11.14	0.266
○	9	1/16	2.234	6.76	0.489
	10		2.267	9.89	0.339
	11		1.828	13.61	0.199
	12		1.891	15.46	0.181
	13		1.932	17.10	0.167
	14		1.960	18.77	0.154
	15		2.000	22.13	0.134
	16		2.015	23.83	0.125
	17		2.029	25.51	0.118
□	18	1/8	1.828	27.60	0.098
	19		1.891	30.75	0.091
	20		1.932	34.05	0.084
	21		1.960	37.58	0.077
	22		1.982	40.90	0.072
	23		2.000	44.23	0.067
	24		2.029	50.83	0.059
	25		2.039	54.13	0.056

FIG. 4. Heated sphere drag at $M \approx 2$; 540° R $< T_w <$ 1860° R. $Re_w = \rho_\infty U_\infty d/\mu_{T=T_w}$.

variable against which to plot C_D was dictated by the fact that the Knudsen number range of the data fell closer to the continuum flow regime than to free-molecule flow; hence, the continuum flow parameter which governs the boundary-layer thickness on the sphere was chosen.

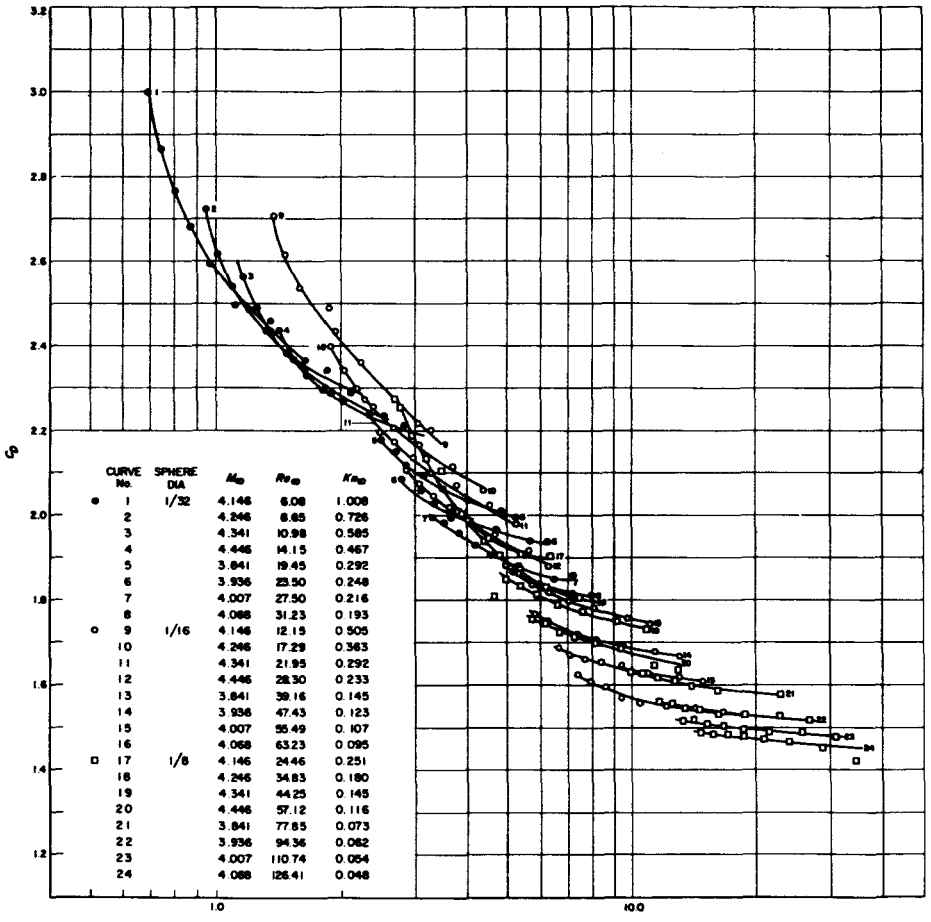

FIG. 5. Heated sphere drag at $M \approx 4$; 520° R $< T_w <$ 1860° R. $\mathrm{Re}_w = \rho_\infty U_\infty d/\mu_{T=T_w}$.

Correlations on the basis of several other logical (and some illogical) parameters have been attempted. Some of these parameters were based on continuum flow hypotheses; e.g.:

(a) The drag increase is due to an increase in pressure or form drag.

That is, the thickening of the boundary layer due to heating results in an increase in the effective sphere diameter, which in turn results in increased pressure drag.

(b) The drag increase is due to increased skin friction. In calculations based on the method of Cohen and Reshotko (1956), as performed by Chahine (1961), attempts were made to evaluate the boundary layer growth with temperature; unfortunately, the work of Cohen and Reshotko, along with countless other boundary layer analyses, fails to treat the case of the hot wall.

Other parameters considered the free-molecular flow aspects, e.g.:

(a) A "wall" Knudsen number, based on the Mach number behind a normal shock wave and the Reynolds number at the wall.

(b) Wall-to-free-stream temperature ratio, singly and in combination with free-stream Mach number.

Suffice to say, none of the approaches outlined above have proved to be of any worth. Some general statements regarding the data may be made.

1. For a given sphere, the increase in drag due to heating becomes greater as the free stream Knudsen number is increased.
2. The low Knudsen number cases, e.g., for the $\frac{1}{8}$ in.-diameter sphere, show only a small drag increase due to heating.
3. There seems to be little Mach number effect, as far as the drag increase due to heating is concerned.
4. Curves at approximately the same Kn_∞ (for differing sphere diameters) do not coincide.
5. Curves at approximately the same Re_∞ (for differing sphere diameters) do not coincide.

The picture is further clouded by the evidence presented in Fig. 6. Here, the $M_\infty \approx 4$ data for three different spheres have been normalized by the equilibrium C_D value and the resulting ratio plotted as a function of wall temperature. The curve shown in the figure has been calculated using the free molecular flow analysis of Schaaf and Talbot (1959). The data for $\mathrm{Kn}_\infty = 0.5$ and 1.0 agree quite well with this calculated curve; that for $\mathrm{Kn}_\infty = 0.25$ falls somewhat below the analysis. This result, if true, is quite surprising, the indication being that, for the sphere, free-molecular flow is achieved when $\mathrm{Kn}_\infty \to 1.0$. Further investigation of this point is under way at the present time.

A comparison of the present data with that of Aroesty (1962) is shown in Figs. 7 and 8. These are included for the sake of completeness, as the

reference data includes measurements for $T_w/T_0 < 1$ while the present data are for $T_w/T_0 > 1$. There is slight disagreement between the two sets of data for $T_w/T_0 = 1$. This writer ascribes some, if not all, of this discrepancy to the tabs of supporting wire depicted in the detail of Fig. 2. Measurements made without these tabs give a slightly lower C_D.

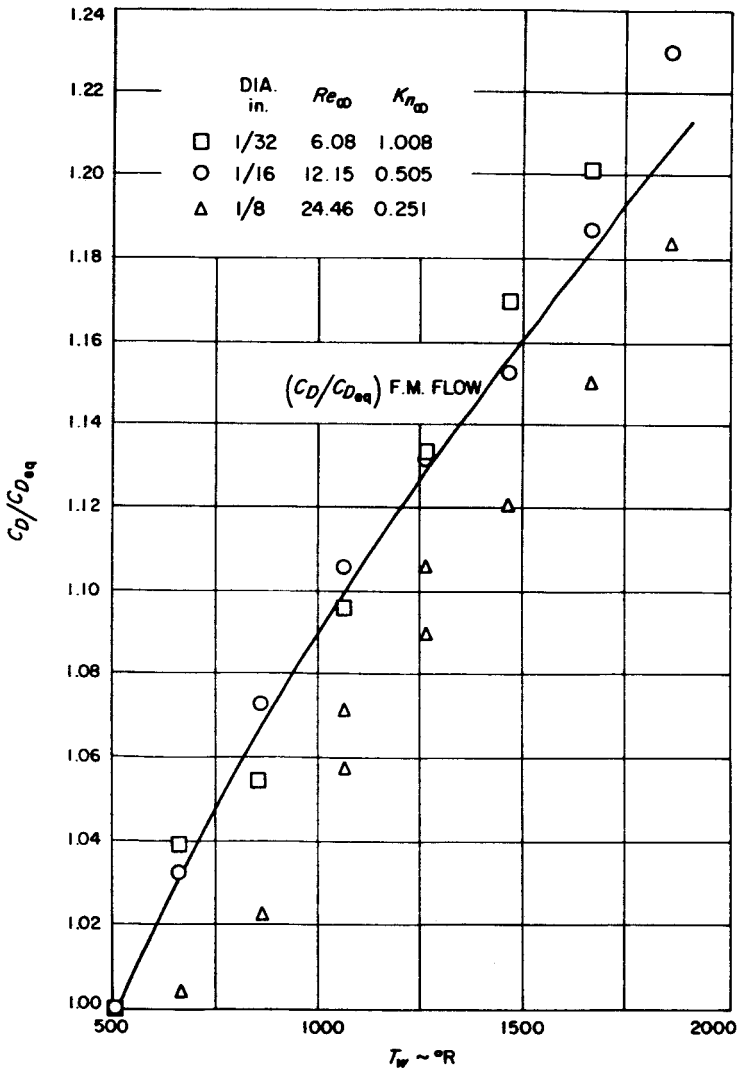

FIG. 6. Drag increase due to heating $M \approx 4.146$.

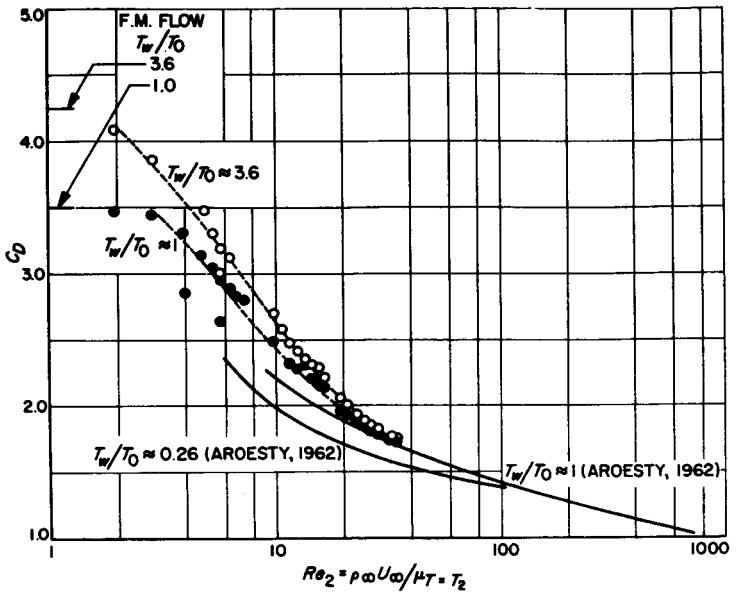

FIG. 7. Effect of wall temperature on drag coefficient. $M \approx 2$.

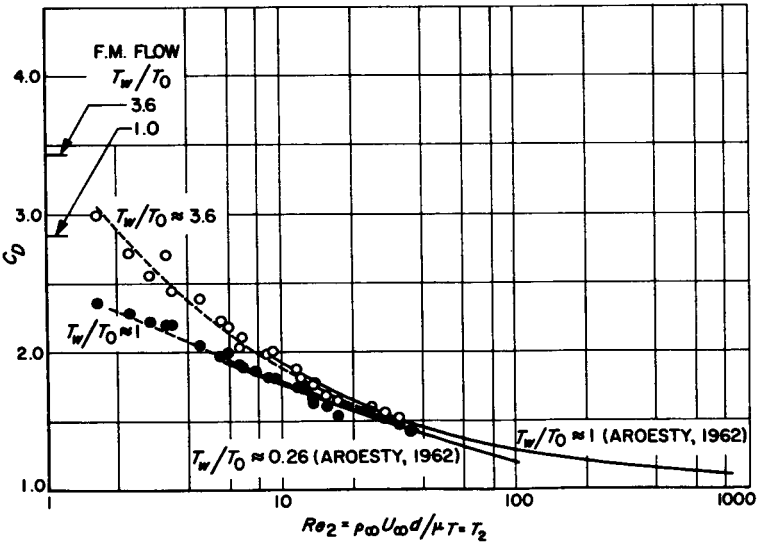

FIG. 8. Effect of wall temperature on drag coefficient. $M = 4$.

ACKNOWLEDGMENT

This paper presents the results of one phase of research conducted at the Jet Propulsion Laboratory, California Institute of Technology under NASA Contract NAsw-7. The author would like to thank Messrs. A. Bouck, S. Neely, and D. Sidwell who assisted in the performance of the experiments. The initial calibrations of several of the nozzles used were performed by Mr. N. Fox. Special notice must be made of the contribution of Mr. H. Geise whose craftsmanship was responsible for the successful construction of the models and suspensions used.

REFERENCES

Aroesty, J. (1962). Univ. Calif. Inst. Eng. Research Rept. HE-150-192; also this volume, p. 261.
Ashkenas, H. (1962). JPL Space Programs Summary No. 37-15, Vol. 4.
Chahine, M. (1961). JPL Research Summary No. 36-8, pp. 82-84.
Cohen, C. B., and Reshotko, E. (1956). NACA TR 1293.
Enkenhus, K. R. (1957). UTIA Rept. 43.
Jensen, N. A. (1951). Univ. Calif. Inst. Eng. Research Rept. HE-150-92.
Kane, E. D. (1951). *J. Aeronaut. Sci.* **18**, 259-270.
Ostriker, J. P., and Davey, J. E. (1960). *Rev. Sci. Inst.* **31**, 570.
Russell, D. A. (1962) JPL Research Summary 36-13, pp. 72-74.
Schaaf, S. and Talbot, L. (1959). Navord Rept. 1488, "Handbook of Supersonic Aerodynamics," Vol. 5, Section 16.
Sherman, F. S. (1951). *J. Aeronaut. Sci.* **18**, 566.
Sreekanth, A. K. (1956). UTIA TN 10.
Sreekanth, A. K. (1961). UTIA Rept. 74.
Wegener, P. P., and Ashkenas, H. (1961)). *In* "Rarefied Gas Dynamics" (L. Talbot, ed.), pp. 663-667. Academic Press, New York.
Wegener, P. P. and Ashkenas, H. (1961b). *J. Fluid Mech.* **10**, 550-560.